Biophysical Journal, Volume *118*

Supplemental Information

Modulation of Kinesin's Load-Bearing Capacity by Force Geometry and the Microtubule Track

Serapion Pyrpassopoulos, Henry Shuman, and E. Michael Ostap

Title: Modulation of kinesin's load-bearing capacity by force geometry and the microtubule track

Authors: Serapion Pyrpassopoulos[1,*], Henry Shuman[1], E. Michael Ostap[1,*].

Affiliations:

[1]Pennsylvania Muscle Institute, Department of Physiology, and the Center for Engineering Mechanobiology, University of Pennsylvania, Perelman School of Medicine, Philadelphia, PA, US.

[*]Correspondence:

serappyr@pennmedicine.upenn.edu or ostap@pennmedicine.upenn.edu

Keywords: Kinesin, microtubules, optical tweezers, single molecule

Supporting Information

Data Analysis

Using the system calibration factor (pN/V) experimental traces were converted to forces. In the three-bead assay the low velocity balance of forces on beads A and B and kinesin K is $\overrightarrow{F_A}(t) + \overrightarrow{F_B}(t) + \overrightarrow{F_K}(t) = 0$, or

$$\overrightarrow{F_K}(t) = -(\overrightarrow{F_A}(t) + \overrightarrow{F_B}(t)).$$

At times before kinesin interacts with the microtubule dumbbell, $\overrightarrow{F_K}(t < t_0) = 0$,

$$\overrightarrow{F_A}(t < t_0) + \overrightarrow{F_B}(t < t_0) = 0$$

and the forces of the two traps are equal and opposite to each other $\overrightarrow{F_A}(t < t_0) = -\overrightarrow{F_B}(t < t_0)$ and their magnitudes equal the pre attachment tensile force on the microtubule ($F_A = F_B = F_{pre\text{-}tensile}$). To reduce any offset or drift errors in the data collection the kinesin force is estimated to be

$$\overrightarrow{F_K}(t) = -[\overrightarrow{F_A}(t) + \overrightarrow{F_B}(t)] - [\overrightarrow{F_A}(t < t_0) + \overrightarrow{F_B}(t < t_0)]$$

$$\overrightarrow{F_K}(t) = -[(\overrightarrow{F_A}(t) - \overrightarrow{F_A}(t < t_0) + (\overrightarrow{F_B}(t) - \overrightarrow{F_B}(t < t_0)]$$

$$\overrightarrow{F_K}(t) = -[\Delta\overrightarrow{F_A}(t) + \Delta\overrightarrow{F_B}(t)]$$

Assuming that the bead-microtubule attachments and the microtubule itself are much stiffer than the two laser traps, the force generated by kinesin

$$\overrightarrow{F_K}(t) = -(k_A + k_B)\,\vec{d}\,(t) \qquad \text{Eq. S1 or}$$

$$\vec{d}\,(t) = -\overrightarrow{F_K}(t) / (k_A + k_B)$$

where k_A and k_B represent the stiffness values of the traps A and B and $\vec{d}$ (t) the displacement of the microtubule dumbbell by kinesin.

The magnitude of the average rate of change of the force $\Delta F_k(t)/\Delta t$ during kinesin's processive runs is:

$$(F_k(t+\Delta t) - F_k(t))/\Delta t = (k_A + k_B) \cdot \Delta d(t)/\Delta t = (k_A + k_B) \cdot v_{av} \qquad \text{Eq. S2}$$

where $v_{av} = \Delta d(t)/\Delta t$ is the average velocity of kinesin for the time interval Δt. From Eq. S2 one can calculate the average velocity of kinesin.

From every dataset we calculate the average trace for kinesin's force production by averaging all kinesin's runs in the dataset. An example of the resulting average force trace is shown in Fig. S4A. The initial rising phase for F < 3 pN is approximated as a linear function of time and from the slope the loading rate dF/dt can be calculated. Then using Eq. S2 the average velocity v_{av} is calculated. The distribution of the mean velocity and the corresponding box statistics, calculated as described above, for different pairs of single beads and surface immobilized microtubules and for different dumbbells are shown in Fig. S4B.

To every statistical quantity q_i, such as median-Δt and v_{av}, calculated for a dataset i, a statistical weight $w_i = n_i/n_{tot}$ is assigned, where n_i represents the number of kinesin runs within dataset i and $n_{tot} = \Sigma n_i$ is the total number of kinesin runs from all datasets of the same assay. The weighted mean $\langle q \rangle_w$ and the weighted standard deviation SD_w of the statistical quantity q are then calculated as follows:

$$\langle q \rangle_w = w_i q_i$$

$$SD_w = \sqrt{\frac{\sum w_i (q_i - \bar{q})^2}{\frac{n_{tot} - 1}{n_{tot}} \sum w_i}}$$

Statistical Comparisons

For statistical comparisons, the non-parametric Wilcoxon-Mann-Whitney test at the 0.05 confidence level was applied using either Origin Software 2018b or Studio R. When the sizes of the two compared datasets were different and the smaller size was characterized by smaller variance, the bigger size dataset was randomly truncated to the same size to avoid adverse effects on the comparison due to significant differences in the variances (38). When comparing more than two datasets with similar variances the non-parametric Kruskal- Wallis test was used.

Imaging Microscopy.

A Leica inverted microscope (DMI3000 B) using a 100 x oil objective from Leica. DIC (Differential interference contrast) microcopy was used to image rectangular parallel ridges. Epifluorescence microscopy was used to image microtubules attached on the ridges shown in Video S1. Further processing of the images was done using imageJ.

Video S1.

Movie of fluorescently labeled microtubules (5% TRITC-tubulin) attached on rectangular ridges with their long axis (4 mm) along the Y-direction and their short axis (2 μm) along the X-direction. Each ridge is 1 μm tall in the Z-direction and 10 μm apart from each other along the X-direction. Images were recorded at a rate of 1 fr/s for 21 seconds.

Video S2.

Cartoon animation showing the positional variability of a streptavidin-bead along the circumference of the microtubule in a dumbbell. The dumbbell is displayed in a cross-sectional view and the azimuthal angle φ between the point of bead attachment and the protofilament that kinesin is interacting is indicated at every frame. The animation is not drawn to scale.

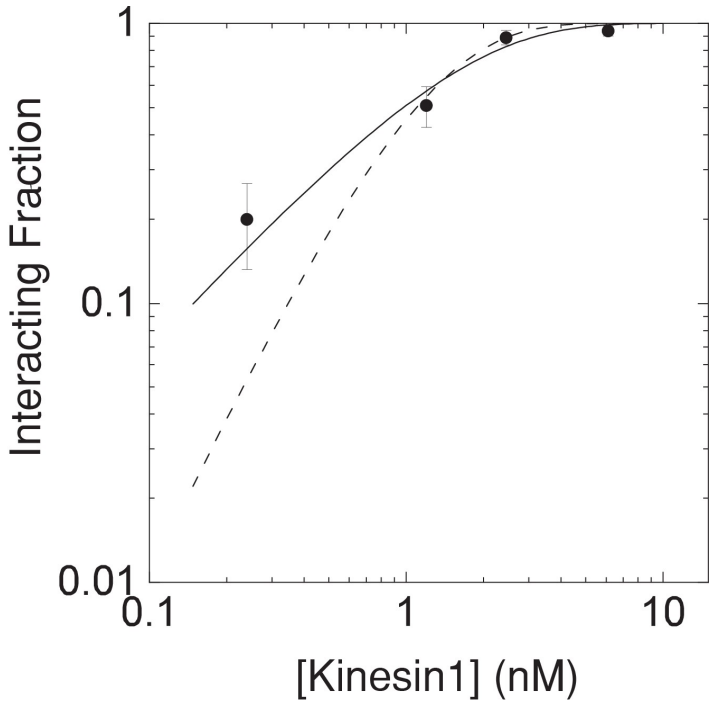

Fig. S1. Single molecule titration for the three-bead assay. The fraction of spherical pedestals that interact with a microtubule dumbbell in the range of 0.2 to 1 as a function of the kinesin concentration x used to decorate the spherical pedestals. For each kinesin concentration N=30 different pedestals were sampled in the same experimental chamber (scatter points). The solid and dashed lines represent fit of the data to the Poisson probabilities that at least one ($P(x) = 1 – \exp(-\lambda x)$) or at least two kinesins dimers ($P(x) = 1 – \exp(-\lambda x) - (\lambda x)\cdot\exp(-\lambda x)$) are interacting with the microtubule dumbbell, correspondingly. P stands for the fraction of interacting pedestals, λ is a fitting parameter and error bars were calculated by the expression $[P(1-P)/N]^{1/2}$. The fit of the solid line ($\chi^2 = 0.012$, $\nu = 3$, $\lambda = 0.71$) is significantly superior compared to the dashed line (reduced $\chi^2 = 7.2$, $\nu = 3$, $\lambda = 1.5$).

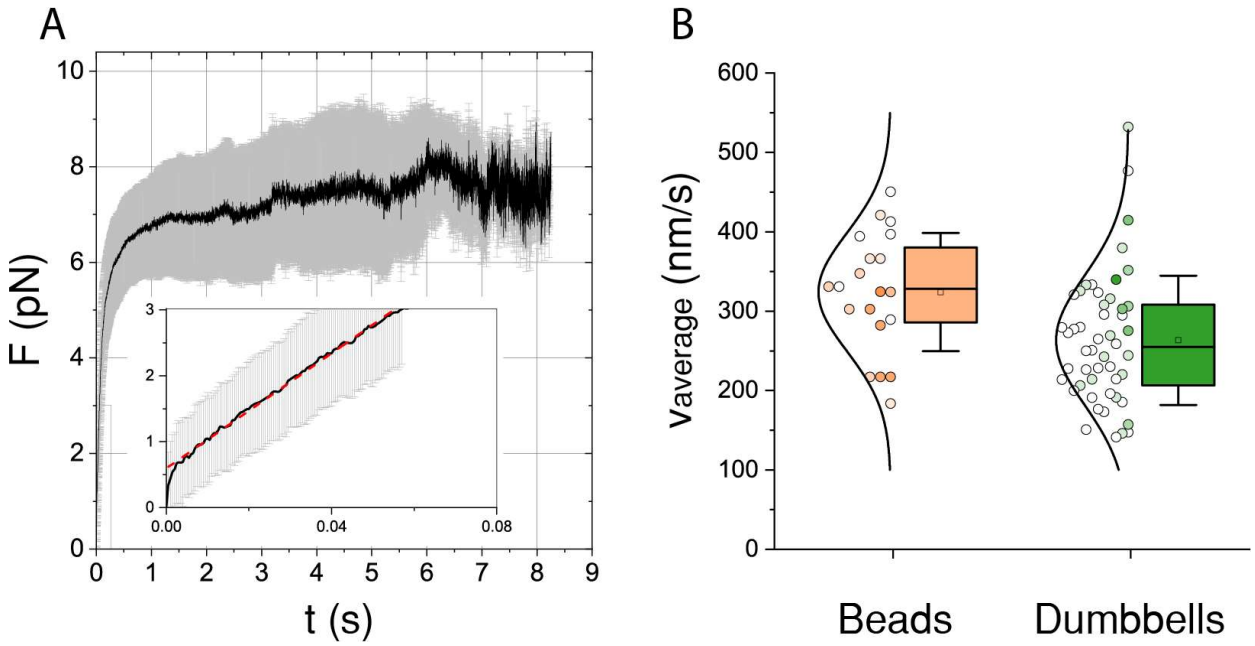

Fig. S2. Average velocity of kinesin for the single-bead and three-bead assays. (A) Examples of the average force trace and the corresponding standard deviation of all kinesin runs from a single dataset are shown by the black line and the gray error bars, respectively. A weighted linear fit (red dashed line) of the initial rising phase for F < 3 pN is shown in the zoom inset. Dividing the slope (pN/s) of the linear fit by the stiffness (pN/nm) the average velocity is calculated (Supporting Information Eq. S2. (B) The distribution of the average velocity and the corresponding box-statistics for 20 different pairs of single beads and surface immobilized microtubules (light brown color) and for 50 different microtubule dumbbells (green color). Each scatter point has been shaded based on its statistical weight, with darker shading indicating higher statistical weight (see Data Analysis).

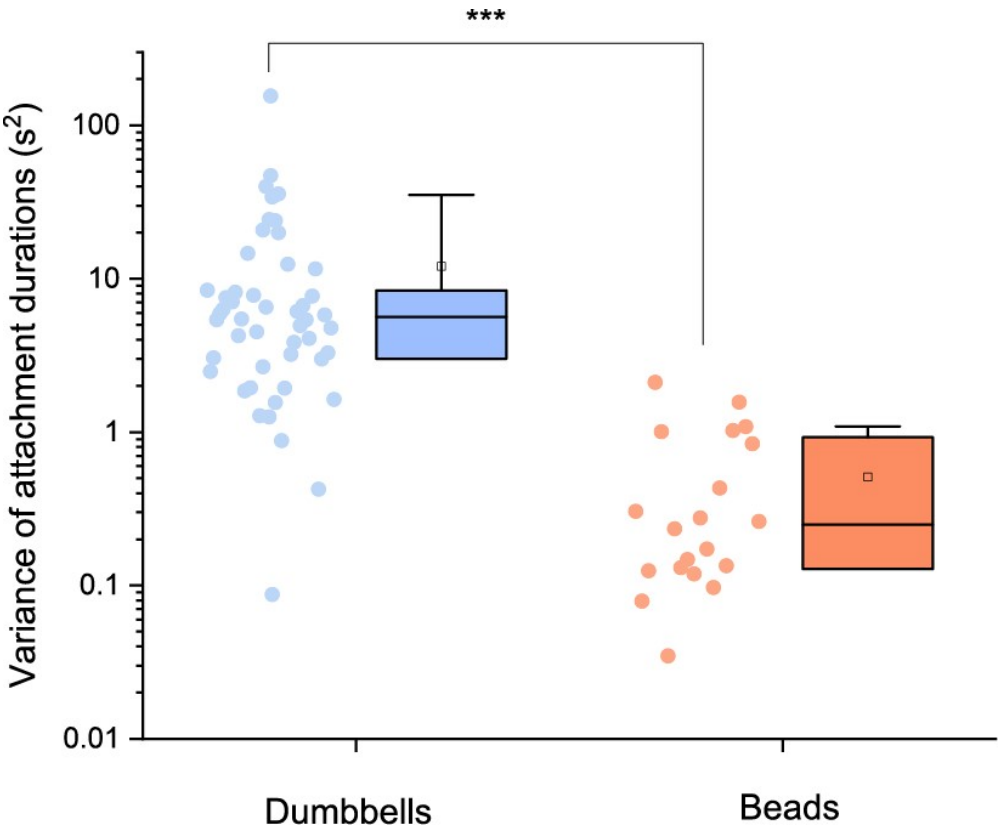

Fig. S3. Distribution of variances for attachment durations in the three-bead and single bead assays.

The distribution of variances of attachment durations (Δt) and the corresponding box statistics is shown for dumbbells (n = 50) and the single beads (n = 20, diam = 0.82 μm). The two distributions are significantly different (Mann-Whitney test, p = 6.2 E-7 < 0.001).

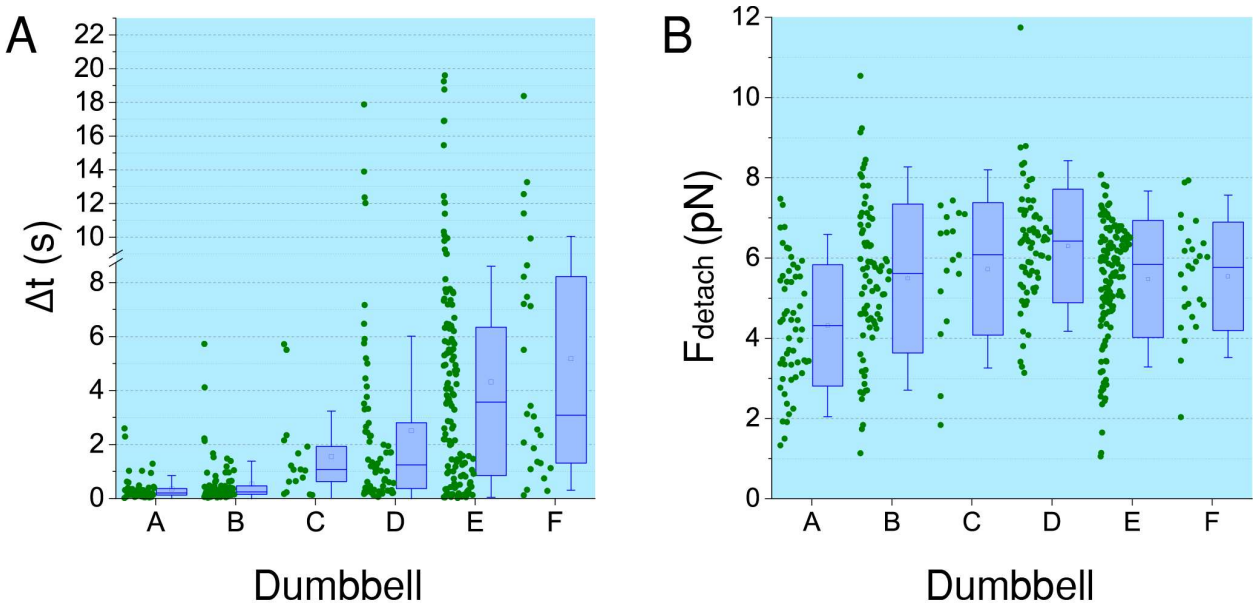

Fig. S4. Distribution of attachment durations and detachment forces between kinesin and GMPCPP microtubules.

Distribution and box statistics of (A) attachment durations Δt and (B) the corresponding detachment forces F_{detach} for single molecule interactions between kinesin and GMPCPP microtubule dumbbells ("A" to "F").

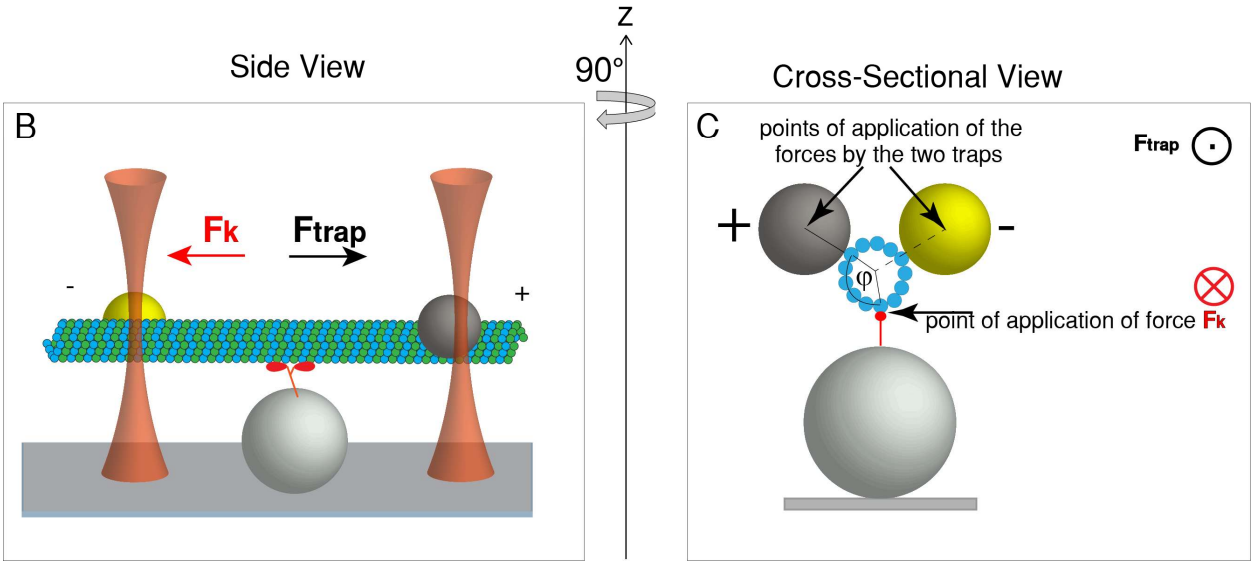

Fig. S5. Cartoon representation (not drawn to scale) of the pair of opposing forces between kinesin and a microtubule dumbbell. (A) The direction of kinesin's motion is towards the plus end (right) and therefore pulls the microtubule towards the opposite direction (left) by applying a force F_k on the interacting protofilament and along the microtubule axis. The stationary laser beams then develop via the trapped beads a net opposing force F_{trap} on the microtubule with its major component along the microtubule axis. (B) Cross-sectional view of relative position of the beads and the interacting kinesin the dumbbell in (A). The relative azimuthal position φ between the attachment point of the plus end bead and interacting kinesin. The major component of F_k is directed vertically towards the back of the page ($\otimes$) and the major component F_{trap} toward the front ($\odot$). The azimuthal separation opposing forces is expected to be variable for the three-bead assay (Video S2).

Table S1.

Different microtubule attachment strategies and substrates for single-bead assay (Fig. 3A)

	Median-Δt (s)	Representation in Fig 2A
Non-Biotinylated MTs immobilized via tubulin Ab on solid surface	0.266	a
	0.425	b
	0.283	c
	0.261	d
Biotinylated MTs immobilized via streptavidin on solid surface	0.315	e
Biotinylated MTs immobilized via streptavidin on Biotinylated lipid bilayer	0.267	f

References

38. Zar, H.J. Biostatistical Analysis. 5th ed. Pearson.